Lab on a Chip

Accepted Manuscript

ROYAL SOCIETY OF CHEMISTRY

www.rsc.org/loc

Journal Name

RSCPublishing

ARTICLE

Engineering fluidic delays in paper-based devices using laser direct writing

Cite this: DOI: 10.1039/x0xx00000x

P. J. W. He, I. N. Katis, R. W. Eason and C. L. Sones

Received 00th January 2012,
Accepted 00th January 2012

DOI: 10.1039/x0xx00000x

www.rsc.org/

We report the use of a new laser-based direct-write technique that allows programmable and timed fluid delivery in channels within a paper substrate which enables implementation of multi-step analytical assays. The technique is based on laser-induced photo-polymerisation, and through adjustment of the laser writing parameters such as the laser power and scan speed we can control the depth and/or the porosity of hydrophobic barriers which, when fabricated in the fluid path, produce controllable fluid delay. We have patterned these flow delaying barriers at pre-defined locations in the fluidic channels using either a continuous wave laser at 405nm, or a pulsed laser operating at 266nm. Using this delay patterning protocol we generated flow delays spanning from a few minutes to over half an hour. Since the channels and flow delay barriers can be written via a common laser-writing process, this is a distinct improvement over other methods that require specialist operating environments, or custom-designed equipment. This technique can therefore be used for rapid fabrication of paper-based microfluidic devices that can perform single or multistep analytical assays.

Introduction

Ever since the first proposal from the Whitesides' group in 2007,[1, 2] the field of paper-based microfluidics has been widely researched and many different lab-on-chip (LOC) type devices have been developed for implementing a wide range of analytical assays. The demand for low-cost alternatives to conventional diagnostic tools has been the driving force that has spurred significant developments in this field. A range of diagnostic assays, ranging from lateral flow type semi-quantitative diagnostic assays to multiplexed tests have already been implemented using such paper-based fluidic devices.[3-6]

Several approaches which include photolithography, [7] followed by wax printing,[8, 9] inkjet printing,[10, 11] plasma oxidation,[12, 13] laser cutting[14] and flexographic printing[15] have been used for fabricating paper-based fluidic devices. We have recently reported the use of a laser-direct-write (LDW) approach for creating fluidic patterns in porous media, namely cellulose paper and nitrocellulose membranes.[16, 17] When compared to alternative techniques, the LDW method presents important advantages: it does not need expensive and fixed patterning masks, custom-modified equipment, specialist chemicals or inks, and it overcomes the limitation on achievable feature size that can result from the lateral spreading of the hydrophobic material used to form the fluidic channel walls.. Finally, and most importantly, it is suitable for scale-up towards mass-production, possibly on a roll-to-roll basis. Using this approach, we have shown that it is possible to fabricate paper-based fluidic devices, which consist of interconnected hydrophilic channels demarcated by hydrophobic polymerised barrier walls that extend through the thickness of the paper, with feature dimensions below a value of 100 μm.

Research into the development of methodologies to control, and in particular delay the flow of fluids in these devices is a much needed requirement that would enable greater functionalities in such paper-based devices. The introduction of control over the transport of fluid could enable a number of other diagnostic detection tests that have multiple timed analytical steps, for example a multistep test such as the enzyme-linked immunosorbent assay (ELISA), which is most often performed under controlled laboratory environments and has a protocol that requires either a machine or skilled personnel to perform the sequential steps at specific time intervals.[18, 19] In addition to this, a number of additional attributes could be incorporated though controllable fluid flow, such as fluidic diodes and valves,[20, 21] timers and metering,[22, 23] fluidic batteries,[24] and such desirable multi-step sample processing sequences have already been reported in the literature.[25, 26]

Current methods that have already been reported for manipulating fluid flow in paper-based fluidic devices can be classified into four main categories: manually activated control,[12, 21] modification of the topology and geometry,[18, 27] addition of dissolvable chemicals,[19, 20] and creation of physical barriers,[28] and each of these procedures has its own advantages, as well as some characteristic limitations. Techniques that use

manually activated control and physical barriers require additional fabrication steps while adding dissolvable chemicals has the dual drawback of additional processing steps and introduction of chemicals such as sugar in the flow-path which might alter or limit the intended function of the devices. Implementation of a similar flow-delay might be possible through careful considerations of the geometry of the fluidic channels. However, to introduce a flow-delay through changes to the channel geometry will require either an increase of the channel dimension or an increase of the channel length, both of which would have the undesired effect of either increasing the foot-print of the device or increasing the volume of the reagents used. Our method instead allows the introduction of flow-delay to any pre-designed device without any change to the channel geometries, thus keep the device compact and requiring smaller reagent volumes.

In this work, to control fluid flow or delivery, we report the use of a new approach that is an extension of the basic LDW technique that we have earlier reported for creating fluidic patterns and devices made up of interconnected channels and reaction chambers. The LDW method (described in references 16 and 17) uses lasers to create fluidic patterns in paper via the light-induced polymerisation of a photopolymer previously impregnated in the paper. Laser-scanning of the paper substrate results in the creation of hydrophobic photopolymer tracks that extend throughout the thickness of the paper, and form the boundary walls of the laser-defined fluidic patterns. To produce flow-control the approach presented here relies on use of physical barriers that run across the flow-path (i.e. perpendicular to the fluidic channels) and hence introduce a delay in the fluid flow. As was the case for our LDW method where we demonstrated the use of laser light to form patterns in paper through light-induced photo-polymerisation, the flow delay barriers in this report are created using the same principle of light-induced photo-polymerisation.

The schematic in Figure 1a shows a simple fluidic geometry that can be used to produce delay barriers via either of the two following methods, (1) by controlling the depth of solid/impermeable barriers (as shown in Figure 1b) that are patterned across the flow and which simply impede the fluid flow by reducing the depth of the fluidic channel or, (2) by forming porous barriers (as shown in Figure 1c) that allow controlled leakage of the fluids. As described and discussed in the later sections, the control over the depth of the barriers of the first type or the porosity of the barriers of the second type is obtained by simply adjusting the laser-writing parameters such as the laser output power and scan speed. Unlike other fluid flow control methods reported for paper-based microfluidics, the approach presented here does not require any additional processing equipment or specialist materials and as described earlier uses the same fabrication approach that defines the fluidic channels themselves.

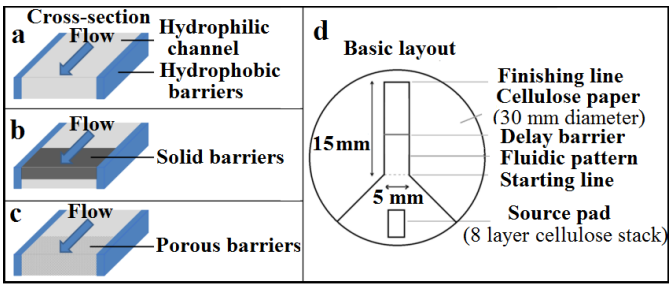

Figure 1 Schematic representation of: a) cross-section of a fluidic channel; b) cross-section of a fluidic channel with solid barriers; c) cross-section of a fluidic channel with porous barriers; d) layout of a pre-defined fluidic structure.

Experimental Section

Laser setups and materials

The lasers used for the direct writing process were a Q-switched Nd: YVO_4 laser (B M Industries, Thomson CSF Laser, France) operating at 266 nm, with a pulse duration of 10 ns, a maximum single pulse energy of 2 mJ, and a repetition rate of 20 Hz (used for method 1 as outlined above, and shown in Figure 1b) and a 405 nm continuous wave (c.w.) diode laser (MLD™ 405 nm, Cobolt AB, Sweden) with a maximum output power of ~110 mW (for method 2, shown in Figure 1c).

The paper substrates used were Whatman® No. 1 filter paper from GE Healthcare Inc. The photopolymer chosen for these experiments was Sub G, from Maker Juice, USA. The sample solution used for characterising the flow delivery delay was Tris Buffered Saline (TBS, 20 mM Tris, pH approx. 7.4, and 0.9% NaCl), which is a buffer commonly used in diagnostic assays. The inks we used for validating the fluid delay in our patterned devices were blue, black and red bottled-inks from Parker, UK.

Creating Fluidic Delays

We first patterned fluidic channels with the design geometry shown in the schematic of Figure 1d, using the LDW technique, which we have previously optimised via a systematic study. The width and length of the fluidic channel was 5 mm and 15 mm respectively, and the inlet end of the channel was designed to replicate the shape of a funnel. These fluidic channel patterns were defined using the c.w. laser operating at 405nm.[17] We subsequently patterned the fluidic barriers within the channels using either of the two lasers described previously.

The channels were patterned using the c.w. laser due to the much higher writing speeds achievable (almost three orders of magnitude greater than that for the pulsed 266 nm source). To ensure that there was sufficient fluid to wick the entire length of the channel, we cut and stacked multiple (8 in this example) pieces of paper (of 3 mm x 5 mm), and positioned them at the wider end of the funnel-shaped inlet of the channel, and loaded

it with a comparatively large volume of fluid (~ 40 µL) – the stack serving as a continuous reservoir of liquid.

During our earlier studies into the fabrication of fluidic channels using pulsed laser irradiation, we observed that by controlling the scanning speed (and therefore the effective exposure) of the laser beam, we could polymerise lines of various depths inside the paper substrate as illustrated schematically in Figure 2a. Slower scanning speeds produced polymerisation through the full depth of the paper, while faster scanning speeds led to photo-polymerisation only in the upper portion of the paper, thus creating partial barriers that the liquid had to overcome. These fluidic 'delay barriers' can therefore decrease the flow by a rate that is proportional to their depth, and hence this principle can be used to impose a user-defined variable time-delay in the wicking of the liquids and test samples.

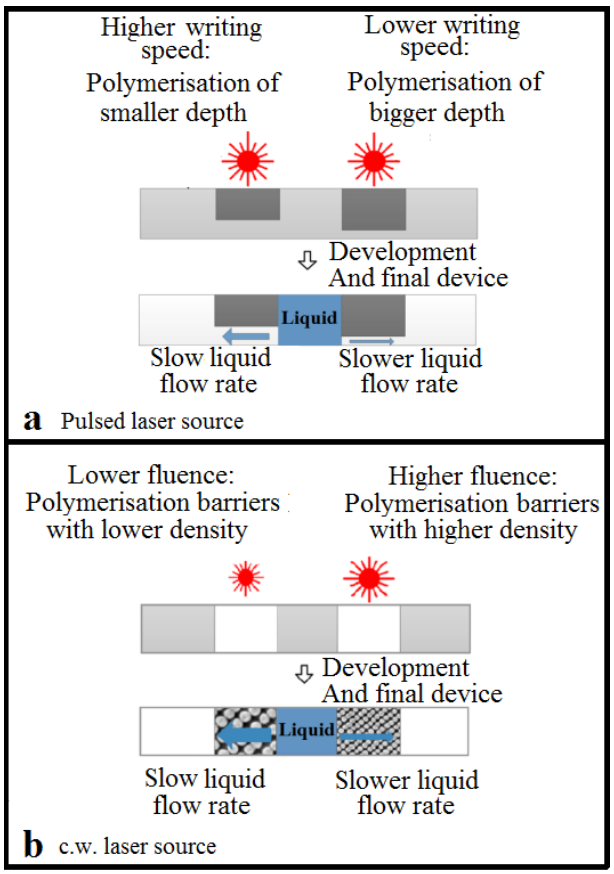

Figure 2 Schematic of the fabrication of polymerised barriers of: a) variable depth inside the paper substrate, created using pulsed laser; b) variable degree of polymerisation extending throughout the full thickness of the paper, created using c.w. laser. Both methods allow for controlled wicking, and variable flow delays.

An alternative approach, as illustrated in Figure 2b allows the writing of barriers via manipulation of the extent or degree of polymerisation using c.w. laser exposure. In this case however, the barriers produced extend throughout the full paper thickness, but the degree of polymerisation can be engineered to form barriers whose porosity can be controlled by varying incident laser fluence, which is determined by the incident laser power and the laser scan speed. For these less dense, leaky barriers, we believe the polymerised material does not completely fill the voids within the paper matrix, thus forming permeable barriers.

Figure 3 illustrates the difference between such solid and porous polymerised barriers. As shown in Figure 3a, the polymerised regions for solid barriers written with a pulsed laser could only be observed on the top, and not the lower face of the paper, suggesting partial polymerisation through the thickness of the paper. However, the polymerised regions for porous barriers written with a c.w. laser always extended throughout the entire paper thickness, as shown in Figure 3b. Blue ink was added to the sample in Figure 3a to enhance the contrast between the paper substrate and the lines.

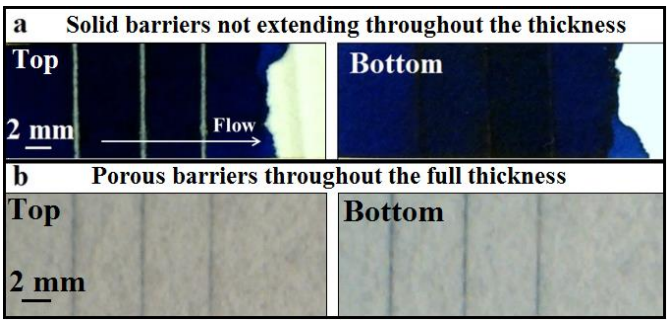

Figure 3 Images showing the delay barriers from both sides of the cellulose paper. a) Depth-variable solid barriers formed by pulsed laser exposure; b) porosity-variable barriers formed by c.w. laser exposure.

As described below, we compare both of these methods for generating controllable flow delay in fluidic channels. The study was aimed at characterising the influence of the laser fluence and exposure on the depths and porosity of the barriers for methods 1 and 2 respectively, including an investigation of delay as a function of positions and numbers of barriers. Since both the fluidic channel walls and delay barriers can be patterned using the same LDW process, this technique should have immediate appeal to manufacturers wishing to develop such paper-based devices on a large scale where production speed and cost are two of the main considerations.

Results and discussion

Method 1: Delay via solid barriers created by pulsed laser writing.

In order to explore the relationship between the depth of the solid barriers and the incident fluence, which depends on both the laser average power and the laser scan speed, we first fabricated a set of polymerised barriers written with a fixed incident average power (7 mW) but different speeds from 0.1

mm/s to 1.5 mm/s. We then measured the depth of these barriers by cutting the paper substrates along a line that intersects the barriers, and then imaged the cross-sections of the paper using an optical microscope. The relationship between the depth and the barrier writing speed is plotted in Figure 4, which shows that an increase in the writing speed from 0.3 mm/s to 1.5 mm/s leads to a decrease in the depth of the barrier from 82 ± 6 % to 17 ± 6 % of the thickness of the paper.

To understand and quantify the usefulness of these solid barriers with variable depths in both delaying and even completely stopping the fluid flow, we fabricated a set of 4 channels, as shown in Figure 5a, and then patterned barrier lines perpendicular to the flow direction. Each of the fluidic channels was inscribed with two barriers, both of which had been written under the same writing conditions. Importantly, for each of the fluidic channels (1 - 4) these pairs of horizontal lines were written with the same incident average power (7 mW) but different speeds namely, 1 mm/s, 0.7 mm/s, 0.5 mm/s and 0.3 mm/s, thus forming solid barriers with differing depths, which can be calculated from the plot in Figure 4.

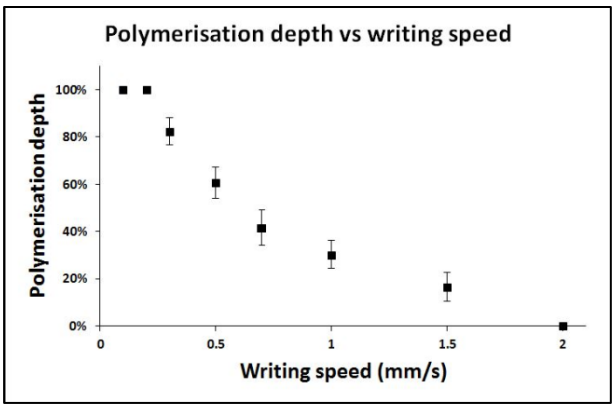

Figure 4 Comparison between the depth of the polymerisation in the paper and the delay barrier writing speed. Error bars indicate the standard deviation for 5 measurements.

As shown in Figure 5b and 5c, blue coloured ink introduced from the inlet of the channels, (marked in the image) experiences a flow rate that is a clear function of the presence and strength of the inscribed barriers, with channel 4 being the slowest, and channel 1 the fastest. The ink was introduced at the same time in each of the four channels. Figure 5b and 5c are images taken 2 minutes and 3 minutes after the introduction of ink, and as seen in Figure 5b, the ink has already flowed past the two barriers of channel 1, is leaking past the second barrier of channel 2, has just reached the second barrier in channel 3, while it has just crossed the first barrier in channel 4.

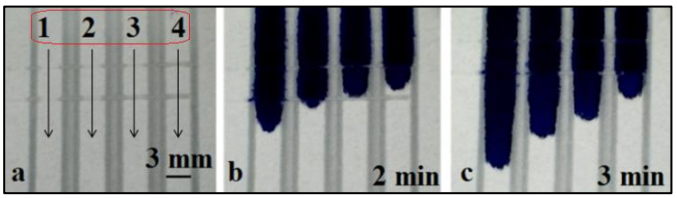

Figure 5 Image showing the delay of the liquid flow after introduction of blue ink in fluidic channels with barriers created using different writing speeds.

To quantify the flow delay versus writing conditions, we used the arrangement of figure 1(d), which is shown in greater detail in Figure 6, using TBS (pH = 7.4), a reagent conventionally used as a buffer in bio-chemical assays, as the liquid medium. The fluid 'delivery time' was defined and measured as the time the TBS solution needed to travel from the starting line to the finishing line, a distance of 15 mm in total. The channel walls were written with the 405 nm c.w. laser (20 mW, 10 mm/s), whereas the barriers were written with a pulsed laser at writing speeds from 1 mm/s to 0.3 mm/s.

First, we studied the consequence of having solid barriers with different depths in the flow-path, however with only one delay barrier at position P1 (as shown in Figure 6a) in each of the pre-defined device. Several devices, each with one single delay barrier were written under different writing conditions, by changing the scan speed (from 1 mm/s to 0.3 mm/s) at a constant laser average power of 7 mW, which corresponded to creation of solid barriers with depths ranging from 30 ± 6 % to 82 ± 6 % of the thickness of the paper (as shown in Figure 4). We have quantified the ability of the barriers to delay the fluid flow using a normalised 'delay factor', which we define as the time to flow (from the starting line to the finishing line) in a channel that has barriers, divided by the time to flow in a channel without barriers:

$$Delay\ factor = \frac{Flow\ time\ for\ a\ channel\ with\ barriers}{Flow\ time\ for\ a\ channel\ without\ barriers}$$

The flow time for the channel with the same geometry as those in Figure 6 but without any barriers is approximately 2 minutes and 40 seconds.

The results for the delay factor are plotted in Figure 7 which show an increase in the delay factor from 1.1 to 1.6 with an increase in the barrier depth from 30 ± 6 % to 82 ± 6 %.

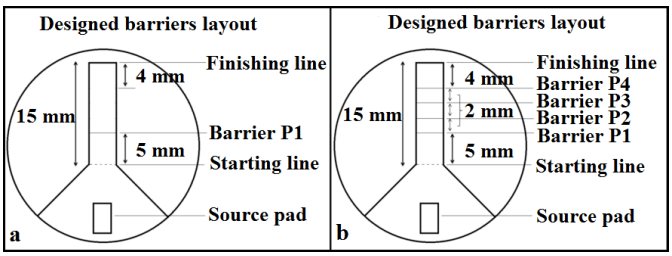

Figure 6 Schematic representation of designed barrier layout showing the position of delay barriers (P1, P2, P3 and P4).

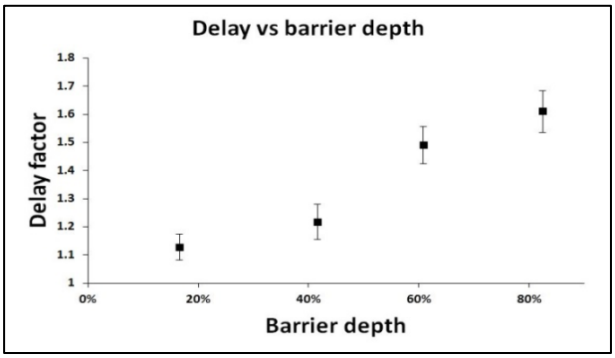

Figure 7 Plots showing the delay factor for devices with barriers having different depths. Barriers were written with different writing speeds at a fixed average power of 7 mW. Error bars indicate the standard deviation for 5 measurements.

Method 2: Delay using porous barriers created by a c.w. laser

In this case, both the fluidic channels and the flow delay barriers were written with the same c.w. laser (in a common programmed writing step) by simply changing either the laser output power or writing speed. To allow for a direct comparison with the results for the solid barriers, fluidic devices that were tested had the same design as in Figure 6.

In this case however, four porous barriers were written across the fluidic channels, to explore the role of number and position of barriers as shown in Figure 6b. A comprehensive study was performed to explore the flow delay induced through barriers written with a range of different writing conditions. The fluid delivery time and the percentage delay were calculated as for method 1.

We first did a comparative study for barriers patterned with different writing conditions, namely different laser powers and scan speeds. Subsequently, we then changed the number of the barriers to explore the relationship between the delay and the number of barriers in the flow path. As in Figure 6b, a one barrier design refers to a device with a single barrier patterned at position P1 in the channel; a two barrier device refers to a channel with two barriers patterned at P1 and P2; and so on.

As shown in Figure 8a, for barriers written with a fixed scan speed of 100 mm/s, the fluid delay gradually increased with an increase of the laser power, and progressively decreased for barriers written with an increasing scan speed at a fixed laser output power of 20 mW, as shown in Figure 8b. These results show that the porosity of these barriers is a clear function of the laser fluence used and that any targeted delay (within the experimental error) can be achieved by choosing the correct fluence. Similarly, for the plots shown in both Figure 8c and 8d, which are based on the use of multiple barriers, we observe identical trends - for barriers written with the same writing conditions, the delay increases with an increase in the number of barriers.

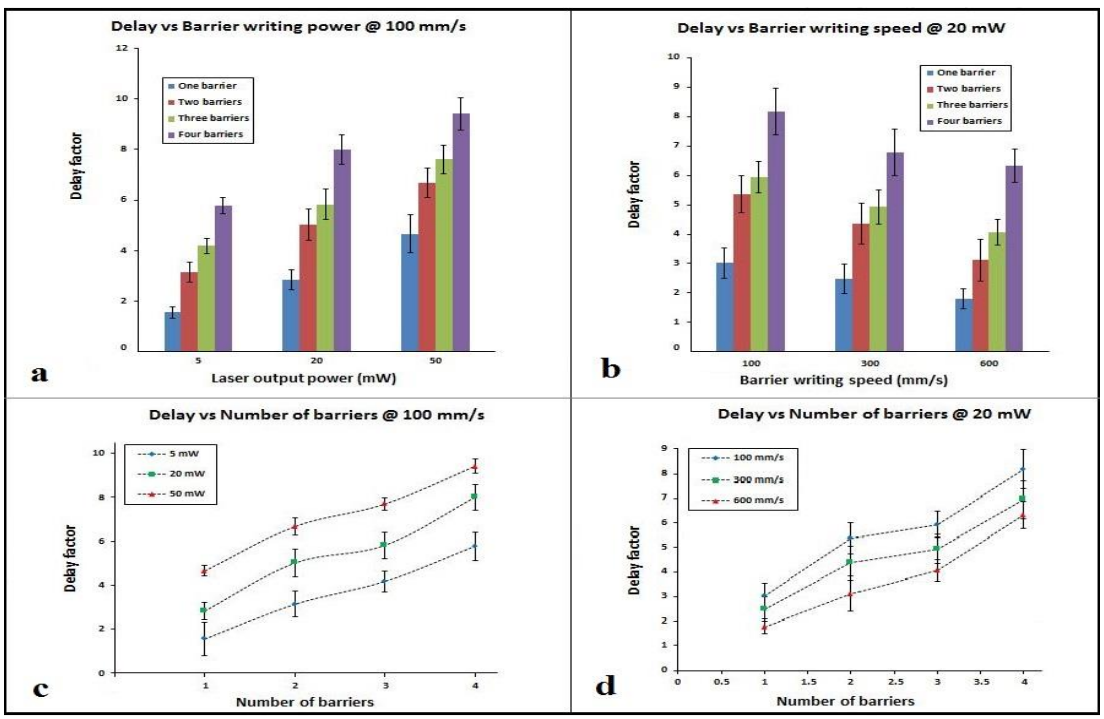

Figure 8 Plots showing the delay factor of delay-barrier-designed devices. a) Barriers written with different laser output powers at a fixed scan speed; b) barriers written with different scan speeds at a fixed laser output power; c) different number of barriers written at a fixed scan speed; d) different number of barriers written at a fixed laser output power. Error bars indicate the standard deviation for 5 measurements, and lines are a simple guide for the eye.

In addition to this dependence on the porosity of the barriers and the number of barriers, we observed that the fluid delay also depended on the position of the porous barrier. We introduced a single porous delay barrier written under the same writing conditions (200 mm/s scan speed and 20 mW laser output power) at different positions (P1 – P4) as show in Figure 6b, and then studied the fluid delay. The plot of the fluid delay versus the position of the porous barrier is shown in Figure 9. As the delay barrier was shifted further from the starting line towards the finishing line, the delay factor rapidly dropped from ~ 2.5 (for position P1) to ~ 1.3 (for position P4). We believe this is because of the geometry of the device, since the volume of the paper that serves as the reservoir for the fluid flow changes with a shift in the position of the delay barrier. The volume before the delay barrier acts as a pump for subsequent flow, thus affecting the flow rate after the barrier. As shown in Figure 6b, the closer the barrier is to the starting line, the smaller the source paper volume is, and this leads, we suggest, to a lower pump force and hence a lower flow rate and larger fluid delay.

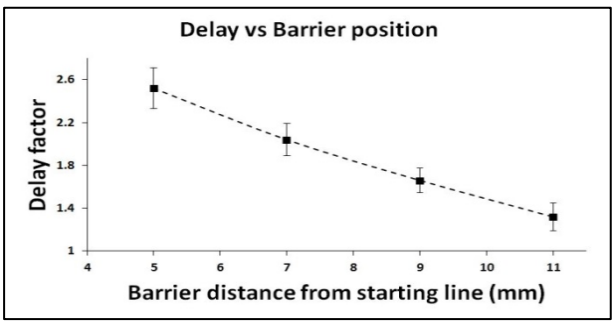

Figure 9 Plots showing the relationship between the fluid delay factor and the position of the delay barriers (distance to the starting line) with the same condition of 200 mm/s scan speed and 20 mW laser output power. Error bars indicate the standard deviation for 5 measurements, and the line is a guide for the eye.

Multiple fluid delivery using delaying barriers

Implementation of automated paper-based devices (as described by Lutz et al.,[19] and Apilux et al.,[18]) that are user-friendly and need minimal intervention from the patient or an unskilled user need strategies that allow control over the flow of several liquids (reagents and sample) along their pathways. Such devices allow the implementation of a multi-step assay (such as an ELISA), and in this section, using fluid delay strategies effected using the flow-barriers described earlier, we demonstrate the usefulness of our method to fabricate such automated paper-based tests. Figure 10 shows a device that uses a network of three identical channels for sequential delivery of three fluids to a common detection or reaction point. As shown in Figure 10, sequential delivery of each of these fluids is made possible by introducing (a set of three identical) porous barriers written with a c.w. laser across the fluid channels. By changing the porosity of each set of delay barriers through simple adjustments of the laser parameters, different delays can be introduced into each channel.

To show the operation of our devices, as also described earlier, we first introduced a source pad (a stack of 8 cellulose papers) into each channel that allows us to load a comparatively large volume of fluid (~ 40 µL) in to each channel, and also serves as a continuous reservoir of liquid (Figure 10). We first tested the performance of our devices using TBS as the test-fluid which was introduced into the source pad in each of the three channels. Figure 10a is a set of images that are snapshots taken sequentially at different times after introducing the TBS into the source pads. The fluid in channel 2 (that does not have any delay barriers) arrived at the intersection zone first (after 5 minutes) and continued to flow onwards until the fluid in channel 3 (with weaker delay barrier) arrived at the intersection (after 10 minutes). Thereafter, the fluids from these two channels mixed and flowed forward until the arrival of the fluid from channel 1 (with the stronger delay barriers) after 20 minutes. Finally, the mixture of three fluids then wicks through the reaction pathway in the following 10 minutes.

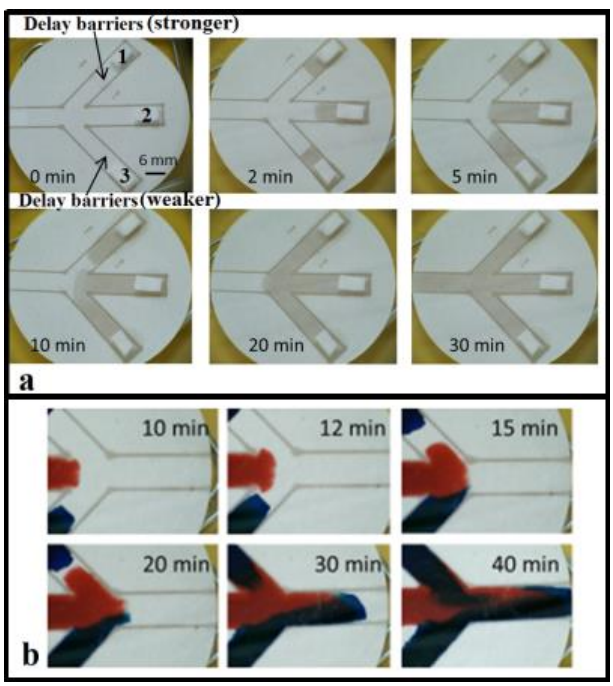

Figure 10 Image showing a 2D multi-channel fluidic device used for sequential delivery of three fluids. It has three identical channels (6 mm width and 23 mm length) modified with different delay barriers (1.Stronger delay barriers; 2. No barriers; 3.weaker delay barriers). a) Sequential images showing the arrival of TBS from each channel at different times; b) Sequential images showing the arrival and mixing of blue and red ink from three separated channel and the subsequent mixing of the inks.

To further illustrate the dynamics related to the mixing of the different fluids and to make the concept of flow delay more obvious, we instead used two different coloured inks to source the three separate channels (blue for channel 1 and 3 and red for channel 2). The sequential images that show the flow through the device are shown in Figure 10b. When compared to the (blank) channel 2 that did not have any delay barriers, the fluid delivery through channel 1 and channel 3 were delayed by 15 and 5 minutes respectively. The results for both of the devices that were either tested using TBS or the coloured inks show clear evidence that our laser-patterned delayed-fluid flow strategy can be used to make paper-based automated devices. As a final step, we demonstrate the use of this strategy to fabricate devices that can implement multi-step ELISA protocols.

Automated multistep assay for CRP detection by sandwich ELISA

This section describes the use of our fluid delay strategy to implement a multiple step ELISA that enables the detection of CRP (C-reactive protein). We have chosen CRP as an example for evaluating this automated paper-based device because it is an important and realistic analyte which is frequently measured for early-stage diagnosis.[29, 30] Devices (with the 2D multi-channel geometries) identical to that shown in Figure 10 were used to realise a multistep enzyme-based immunoassay that allowed for the detection of CRP. As shown in Figure 11a, the three individual arms of the device were used to sequentially deliver the three different reagents - channel 1 delivered streptavidin-HRP; channel 2 delivered the sample; channel 3 delivered the detection antibody through to the capture antibody which was immobilized in the detection zone (identified in the image with a rectangular frame). As mentioned earlier, the device geometry and the delay mechanism used were the same as those in Figure 10, except that an additional cellulose absorbent pad was attached at the end of the detection pathway for collection of the excess fluid.

The ELISA kit used in the implementation of the CRP detection (DuoSet® Human C-Reactive Protein/CRP) was purchased from R&D Systems, Inc. (UK). All the antibodies used were from this kit and were diluted to the working concentrations of 3.6 µg/mL and 162 ng/mL for capture antibody and conjugated antibody respectively. The CRP human standard (C1617) was purchased from Sigma-Aldrich (UK) and diluted to working concentrations using calibrator diluent (1% BSA in PBS).

The capture antibody was pipetted at four distinct spots (1 µL per spot) within the detection zone, and then left to dry for one hour at room temperature. The whole device was then immersed in a blocking solution (5 % BSA in PBS) for one hour at room temperature, followed by three sequential washing steps using PBS. After subsequent drying, the device was ready to use.

In order to implement the assay, 40 µL of each reagent was sequentially pipetted onto the source pads within a period of a few seconds in each channel and the device was left in a covered petri dish at room temperature to allow for the timed, sequential delivery of the individual solutions along each channel, into the detection zone for reaction with the capture antibodies immobilized therein. The devices were held along their edges by a specially designed holder that suspended them in air thus eliminating any contact with the petri dish surface underneath which otherwise would have altered the flow of the reagents. After 30 minutes, the whole device was washed three times using PBS for five minutes each. Finally, 10 µL of the colorimetric substrate TMB (Tetramethylbenzidine) was added at the detection zone and the result was read after 20 minutes. Ideally, such a device should also enable the sequential delivery of TMB to the detection zone via another fluid flow channel, and that would then be a true example of a sample-in-result-out type device, however, for this initial proof-of-principle experiment where we intend to show the usefulness of delays, we have not yet manufactured such a test. In the case of several routinely employed assays, the detection antibodies are tagged either with a gold nanoparticle or coloured beads, and if we choose to use detection antibodies labelled in this fashion, then there would not be the need to have this additional delivery path. Figures 11b, 11c and 11d show the results for the detection of different concentrations of CRP, and the clearly visible and distinct blue spots that appear in the detection zone (with minimal background colour 'noise') confirm the presence of CPR in the sample. Figure 11e shows the result for a control device tested with a sample solution that did not have CRP. As shown in the figure, for this negative result, we do not observe any specific blue spots in the detection zone. The colour intensity of the spots in Figure 11b is greater than that in Figure 11c, and this relates to the higher concentration of CRP in the corresponding samples that were used in the two different cases. For some of the spots, their non-symmetric circular shape is as a result of the spotting of the capture antibodies more towards one edge of the channel walls, resulting in a clipping of their circular shape. The images in Figure 11b and 11c clearly demonstrate the successful detection of CRP on our laser-patterned paper-based device with incorporated fluid delay mechanisms. This device is an example of a semi-automatic type test that still requires intervention from a user, but we are planning on developing this concept further in the immediate future to enable a fully-automated device which would then be a true example of a sample-in-result-out type device. In addition, using our devices, we were also able to detect CRP with concentrations of less than ~ 10 ng/mL, which we believe is close to the limit of detection.

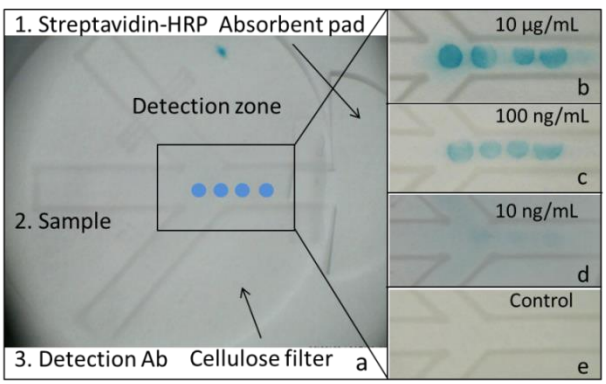

Figure 11 Automated multi-step ELISA for CRP detection in a 2D multi-channel fluidic device. a) Image of a device showing its design and indicating reagent locations for the assay. Four blue spots, shown schematically in a), represent the position of immobilized capture antibody in the detection zone. b), c), d) and e) are photos of the CRP ELISA result on the device for different sample concentrations of 10 µg/mL, 100 ng/mL, 10 ng/mL and no sample respectively.

Conclusions

In this work, we report a new method based on our LDW technique that allows the fabrication of pre-programmed or timed fluid delivery in paper-based fluidic devices without any additional equipment or minimal actions from the user. Barriers, aligned perpendicular to the flow-path, and used to control the fluid flow in a channel were either solid barriers with differing depths, or barriers with differing porosity, and these could be fabricated by simple adjustments of the laser patterning parameters, such as the laser power and the writing speed. Both types of barriers yield similar results for control over the fluid flow. These programmable fluid delay techniques should help to further improve the functionalities of paper-based microfluidic devices as such control can be used to enable semi-automated multi-step fluidic protocols. In contrast to other methods reported for controlling fluidic transport, our approach eliminates the requirements for cleanroom-based steps, or custom-designed equipment, or the need for long flow paths, which can then translate into requirements for larger analyte volumes. Most importantly, since the delay-mechanism can be an integral part of the fabrication of the fluidic devices themselves, we believe this integrated process presents a considerable manufacturing and hence commercial advantage. With our existing laser-writing set-up, it is possible to pattern devices, using a c.w. laser, at speeds of a metre per second, and accounting for the time required for the pre and post processing steps needed to make a complete device, our estimate is that it is possible to fabricate at least one device per second. Above all, we believe that this method could be an ideal choice for rapid fabrication of custom-designed paper-based microfluidic devices for realizing single or multistep analytical tests.

Acknowledgements

The authors acknowledge the funding received via the Engineering and Physical Sciences Research Council (EPSRC) Grant Nos. EP/J008052/1 and EP/K023454/1, and the funding received via a Knowledge Mobilisation Fellowship for Dr. Collin Sones from the Institute for Life Sciences and the Faculty of Health Sciences of the University of Southampton. The data for this paper can be found at 10.5258/SOTON/377463.

Notes and references

[a] *Optoelectronics Research Centre, University of Southampton, Highfield, Southampton, U.K. SO17 1BJ. Tel:44 2380 599091; E-mail: ph3e12@soton.ac.uk*

1. A. W. Martinez, S. T. Phillips, M. J. Butte and G. M. Whitesides, *Angew. Chem.-Int. Edit.*, 2007, **46**, 1318-1320.
2. A. W. Martinez, S. T. Phillips and G. M. Whitesides, *Proc. Natl. Acad. Sci. U. S. A.*, 2008, **105**, 19606-19611.
3. I. N. Katis, J. A. Holloway, J. Madsen, S. N. Faust, S. D. Garbis, P. J. S. Smith, D. Voegeli, D. L. Bader, R. W. Eason and C. L. Sones, *Biomicrofluidics*, 2014, **8**, 9.
4. A. W. Martinez, S. T. Phillips, G. M. Whitesides and E. Carrilho, *Anal. Chem.*, 2010, **82**, 3-10.
5. E. Carrilho, S. T. Phillips, S. J. Vella, A. W. Martinez and G. M. Whitesides, *Anal. Chem.*, 2009, **81**, 5990-5998.
6. X. Li, D. R. Ballerini and W. Shen, *Biomicrofluidics*, 2012, **6**, 13.
7. A. W. Martinez, S. T. Phillips, B. J. Wiley, M. Gupta and G. M. Whitesides, *Lab Chip*, 2008, **8**, 2146-2150.
8. E. Carrilho, A. W. Martinez and G. M. Whitesides, *Anal. Chem.*, 2009, **81**, 7091-7095.
9. V. Leung, A. A. M. Shehata, C. D. M. Filipe and R. Pelton, *Colloid Surf. A-Physicochem. Eng. Asp.*, 2010, **364**, 16-18.
10. X. Li, J. F. Tian, G. Garnier and W. Shen, *Colloid Surf. B-Biointerfaces*, 2010, **76**, 564-570.
11. J. L. Delaney, C. F. Hogan, J. F. Tian and W. Shen, *Anal. Chem.*, 2011, **83**, 1300-1306.
12. X. Li, J. F. Tian, T. Nguyen and W. Shen, *Anal. Chem.*, 2008, **80**, 9131-9134.
13. C. D. Souza, O. C. Braga, I. C. Vieira and A. Spinelli, *Sens. Actuator B-Chem.*, 2008, **135**, 66-73.
14. E. Fu, P. Kauffman, B. Lutz and P. Yager, *Sens. Actuator B-Chem.*, 2010, **149**, 325-328.
15. J. Olkkonen, K. Lehtinen and T. Erho, *Anal. Chem.*, 2010, **82**, 10246-10250.
16. P. J. W. He, I. N. Katis, R. W. Eason and C. L. Sones, *Biomicrofluidics*, 2015, **9**, 26503-26503.
17. C. L. Sones, I. N. Katis, P. J. W. He, B. Mills, M. F. Namiq, P. Shardlow, M. Ibsen and R. W. Eason, *Lab Chip*, 2014, **14**, 4567-4574.
18. A. Apilux, Y. Ukita, M. Chikae, O. Chailapakul and Y. Takamura, *Lab Chip*, 2013, **13**, 126-135.
19. B. Lutz, T. Liang, E. Fu, S. Ramachandran, P. Kauffman and P. Yager, *Lab Chip*, 2013, **13**, 2840-2847.
20. H. Chen, J. Cogswell, C. Anagnostopoulos and M. Faghri, *Lab Chip*, 2012, **12**, 2909-2913.
21. A. W. Martinez, S. T. Phillips, Z. H. Nie, C. M. Cheng, E. Carrilho, B. J. Wiley and G. M. Whitesides, *Lab Chip*, 2010, **10**, 2499-2504.
22. H. Noh and S. T. Phillips, *Anal. Chem.*, 2010, **82**, 8071-8078.
23. H. Noh and S. T. Phillips, *Anal. Chem.*, 2010, **82**, 4181-4187.
24. N. K. Thom, K. Yeung, M. B. Pillion and S. T. Phillips, *Lab Chip*, 2012, **12**, 1768-1770.
25. J. L. Osborn, B. Lutz, E. Fu, P. Kauffman, D. Y. Stevens and P. Yager, *Lab Chip*, 2010, **10**, 2659-2665.
26. E. L. Fu, S. Ramsey, P. Kauffman, B. Lutz and P. Yager, *Microfluid. Nanofluid.*, 2011, **10**, 29-35.
27. E. Fu, B. Lutz, P. Kauffman and P. Yager, *Lab Chip*, 2010, **10**, 918-920.
28. D. L. Giokas, G. Z. Tsogas and A. G. Vlessidis, *Anal. Chem.*, 2014, **86**, 6202-6207.
29. T. B. Ledue and N. Rifai, *Clin. Chem. Lab. Med.*, 2001, **39**, 1171-1176.
30. N. Rifai, R. P. Tracy and P. M. Ridker, *Clin. Chem.*, 1999, **45**, 2136-2141.

